

Digitizer of astronomical plates at Shanghai Astronomical Observatory and its performance test

Yong Yu, Jian-Hai Zhao, Zheng-Hong Tang, Zheng-Jun Shang

Shanghai Astronomical Observatory, Chinese Academy of Sciences, Shanghai 200030, China; yuy@shao.ac.cn

Received 2016 November 4; accepted 2016 December 27

Abstract Before CCD detectors were widely employed in observational astronomy, the main method of detection was the use of glass astrophotographic plates. Astronomical plates have been used to record information on the position and activity of celestial bodies for more than 100 years. There are about 30 000 astronomical plates in China, and the digitization of astronomical plates is of great significance for permanent preservation and to make full use of these valuable observation data. A digitizer with high precision and high measuring speed is a key piece of equipment for carrying out the task of digitizing these astronomical plates. A digitizer for glass astrophotographic plates was developed jointly by Shanghai Astronomical Observatory and Nishimura Co., Ltd of Japan. The digitizer's hardware was manufactured by Nishimura Co., Ltd, and the performance test, error corrections as well as image processing of the digitizer were carried out by Shanghai Astronomical Observatory. The main structure and working mode of the digitizer are introduced in this paper. A performance test shows that brightness uniformity of illumination within the measuring area is better than 0.15%, the repeatability of digitized positions is better than 0.2 μm and the repeatability of digitized brightness is better than 0.01 instrumental magnitude. The systematic factors affecting digitized positions, such as lens distortion, the actual optical resolution, non-linearity of guide rails, non-uniformity of linear motors in the mobile platform, deviation of the image mosaic, and non-orthogonality between the direction of scanning and camera linear array, are calibrated and evaluated. Based on an astronomical plate with a size of 300 mm \times 300 mm, which was digitized at different angles, the conversion residuals of positions of common stars on different images were investigated. The results show that the standard deviations of the residuals are better than 0.9 μm and the residual distribution is almost random, which demonstrates the digitizer has a higher precision for digitization.

Key words: astrometry — instrumentation: detectors — methods: data analysis — techniques: image processing

1 INTRODUCTION

Before CCD detectors were widely employed in observational astronomy, the main method of detection was the use of glass astrophotographic plates. Astronomical plates contain information on the position and activity of celestial bodies spanning more than 100 years, and they represent a non-reproducible record of observations. The information on astronomical plates can be used not only as a basis for modern CCD observations, but also in some astronomical research, such as solar dy-

namics (Kavelaars 2004), stellar kinematics (Høg et al. 2000), long-period binary stars, multiple-star system dynamics (Torres & Stefanik 2000) the light variability of celestial bodies with long time scales (Fresneau et al. 2001), and so on. According to statistics, there are about 30 000 astronomical plates in China. At present, most of these plates have been centrally preserved in Sheshan Astronomical Plate Library of Shanghai Astronomical Observatory.

Due to their special physical and chemical properties, astronomical plates are very hard to preserve. Once

the preservation conditions are not ideal, astronomical plates are prone to mildewing, film falling off, or even scrapping entirely. In addition, the vast majority of these astronomical plates have not been digitized yet, which restricts the value of observational data they might contain. Therefore, the digitization of astronomical plates is extremely significant for permanent preservation and making full use of these valuable observations. Thus the International Astronomical Union (IAU), since 2000, has had a working group dedicated to the Preservation and Digitization of Photographic Plates (PDPP). This working group asked all observatories around the world to digitize their plates as soon as possible. As a result, a project was launched in China in 2012 to digitize the 30 000 plates available at all Chinese observatories in the following five years. A digitizer for glass astrophotographic plates, with high precision and high measuring speed, is a key piece of equipment needed to carry out this project.

In the past, domestic scholars have adopted a Photometric Data Acquisition System (PDS) to collect information contained in some astronomical plates (Yan *et al.* 1986, Mao *et al.* 1993, Wang *et al.* 1996). However, the measuring speed of a PDS is very slow and it would take several hours (depending on size) to measure a plate, which limits the application of PDS in digitizing astronomical plates. Using a commercial scanner to digitize astronomical plates seems to be a simpler approach, but the measurement accuracy of commercial scanners is difficult to guarantee. Especially in the scanning direction of a commercial scanner, there are random errors of several microns and systematic errors of tens of microns (Yan *et al.* 2016). In order to improve the efficiency and accuracy of the digitization, in last ten years, Harvard College Observatory and Belgian Royal Observatory have both developed digitizers for astronomical plates (Simcoe *et al.* 2006, de Cuyper & Winter 2006). Both digitizers use the method of block scanning to take a series of frames of the plate which are then stitched together in a mosaic to create an image of the whole plate. They are equipped with an XY-table that has an air bearing and linear motor, with micron accuracy, a doublesided telecentric lens and a stable light system composed of LED arrays, so as to ensure the quality of digitization in astronomical plates.

Since 2013, Shanghai Astronomical Observatory and Nishimura Co., Ltd of Japan have jointly developed a new digitizer for glass astrophotographic plates. Nishimura Co., Ltd manufactured the digitizer hardware, and the performance test, error corrections as

well as image processing of the digitizer were carried out by Shanghai Astronomical Observatory. After two years of development, the machine achieved a precision of better than $1\ \mu\text{m}$ in digitization position, and 10 minutes are needed to digitize a plate with dimensions of $300\ \text{mm} \times 300\ \text{mm}$, which meet the requirement for digitization of astronomical plates. In Section 2, we present the main structure and working mode of the digitizer. The tests of the digitizer's performance are described in Section 3. Section 4 presents some conclusions.

2 MAIN STRUCTURE AND WORKING MODE OF THE DIGITIZER

The digitizer is situated in the inner laboratory of Sheshan Astronomical Plate Library and it is composed of a linear array camera, a doublesided telecentric lens, a mobile platform, an LED light system, etc., which are integrated and mounted on a marble platform that weighs 900 kg, as shown in Figure 1. In order to avoid the influence of vibrations caused by movements of the operator during the measurement process, the marble platform is placed on an independent cement base and isolated with an outer layer. The cement base is embedded in the rock layer of Sheshan Mountain. Sheshan Astronomical Plate Library always maintains an environment with constant temperature (25°C) and constant humidity (50%). The digitizer is covered with a customized plastic sheeting room, as shown in Figure 2, to further reduce the impact of airflow from the indoor air conditioning on the movement of the mobile platform.

Different from the working mode adopted by digitizers at Harvard College Observatory and Belgian Royal Observatory, the digitizer at Shanghai Astronomical Observatory uses the method of line scanning. During the measurement process, the camera and LED light system remain stable, and the mobile platform drives one astronomical plate to undergo uniform linear motion along the scanning direction (Y). At the same time, the linear array camera is continuously exposed to collect information on the plate. The camera array is 2880 pixels in size, and the pixel size is $10\ \mu\text{m}$, which makes the width of a single data acquisition 28.8 mm. The total distance moved in the scanning direction is 350 mm. In order to complete the process of acquiring information over the whole astronomical plate, the mobile platform needs to drive the plate to do multiple step motions of length 28.8 mm in the stitching direction (X). This measurement is done continuously for each step motion until the whole plate is

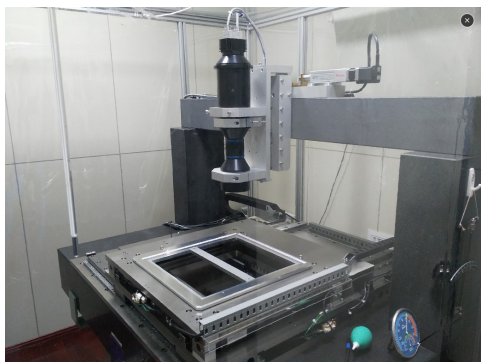


Fig. 1 Photo of the digitizer for astronomical plates at Shanghai Astronomical Observatory.

covered. For example, the largest plates in the Sheshan Astronomical Plate Library are about $300\text{ mm} \times 300\text{ mm}$ in size, and it will take at least nine steps of this motion to cover the whole plate. Finally, image mosaic technology is used to stitch all the strip images into a whole image. The entire process takes about 10 minutes.

3 PERFORMANCE TEST OF THE DIGITIZER

After the digitizer was developed in 2016, we carried out a test of its performance. The test included illumination non-uniformity within the measuring area, digitizing repeatability, systematic factors affecting the digitized positions, as well as a comprehensive test on the precision of the digitized positions. Test tools include: (1) A glass calibration plate produced by the Edmund Optics Company. Its effective size is $50\text{ mm} \times 50\text{ mm}$ and there are 201×201 standard dots distributed evenly. The dot spacing is 0.25 mm and the positional accuracy is $1\text{ }\mu\text{m}$. (2) The astronomical plate used in the test was taken by a 40 cm telescope in 1981 at Beijing Astronomical Observatory (plate number is DA2849). Its size is $300\text{ mm} \times 300\text{ mm}$ and there are about 3500 stars on the plate.

3.1 Illumination Non-Uniformity

The astronomical plate is digitized by means of transmission measurement, which requires illumination within the measuring area to be as uniform as possible. In order to test the quality of illumination, an area of $288\text{ mm} \times 288\text{ mm}$ was measured without placing any plate to obtain an image. The image was divided evenly into 20×20 regions and Figure 3 shows the distribution of the average grey value of each region. The maximum, minimum and mean values are

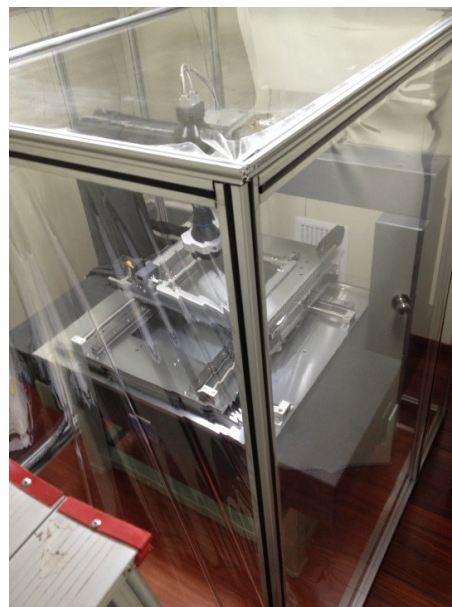


Fig. 2 Digitizer is covered with customized plastic sheeting to reduce the impact of airflow from the indoor air conditioning.

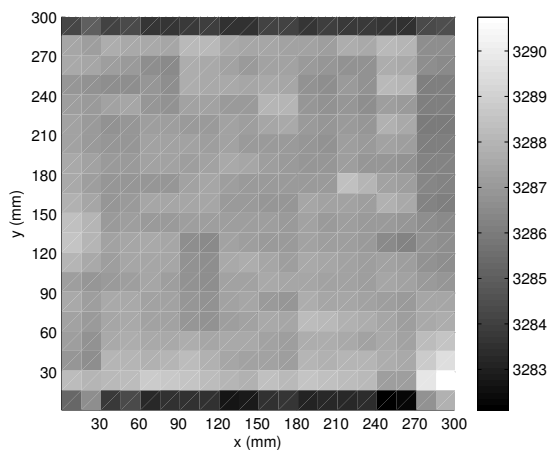


Fig. 3 Distribution of the average grey value of each region within a measuring area of $288\text{ mm} \times 288\text{ mm}$.

3290.7 ADU , 3282.1 ADU and 3287.0 ADU respectively. Here $\frac{|\text{maximum}-\text{mean}|}{\text{mean}}$ and $\frac{|\text{minimum}-\text{mean}|}{\text{mean}}$ are used to evaluate the illumination non-uniformity, and our results indicate that illumination non-uniformity within the measuring area is better than 0.15%. From Figure 3, it can also be seen that the darker regions are concentrated in the upper and lower edges of the image, which might be due to shading of the plate holder with respect to the LED light.

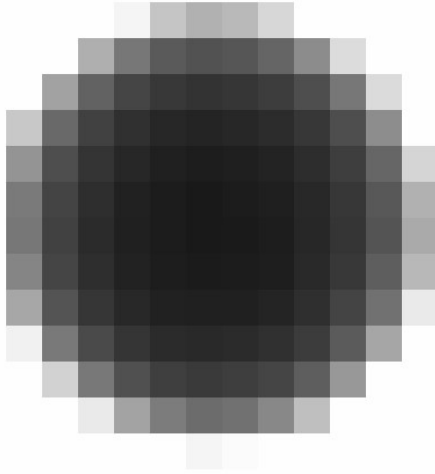


Fig. 4 Example of a standard dot on the Edmund Optics calibration plate.

3.2 Digitizing Repeatability

Digitizing repeatability is consistency among successive digitizations of the same object under the same condition, which reflects the internal accuracy of the equipment. A direct test of digitizing repeatability is to measure a plate repeatedly and calculate the standard deviation of the measured coordinates and brightnesses of the stars in multiple images. The standard deviation can reflect the digitizing repeatability. In order to reduce the influence of centering and photometric errors, an ideal scheme is using the digitized image of the calibration plate, since an image of a standard dot on the calibration plate is symmetrical with a higher signal-to-noise ratio, as shown in Figure 4, which can ensure higher centering and photometric accuracy. However, the calibration plate is only $50\text{ mm} \times 50\text{ mm}$ and cannot cover the entire measuring range, so we also use an astronomical plate with a size of $300\text{ mm} \times 300\text{ mm}$ to test digitizing repeatability.

Both the $50\text{ mm} \times 50\text{ mm}$ calibration plate and the $300\text{ mm} \times 300\text{ mm}$ astronomical plate were digitized and measured repeatedly five times. The standard deviations of the residuals of the measured coordinates and the brightnesses for all standard dots and stars on the plates were calculated.

Figures 5 and 6 display histograms of the standard deviations of the residuals of the measured coordinates in X and Y expressed in μm , and of the brightness expressed in instrumental magnitude, for all standard dots and stars respectively.

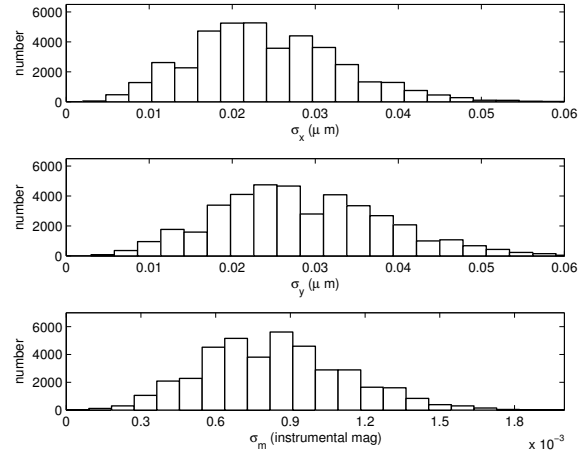


Fig. 5 Histogram of the standard deviations of the residuals of the measured coordinates and brightnesses for all standard dots on the standard plate with a size of $50\text{ mm} \times 50\text{ mm}$.

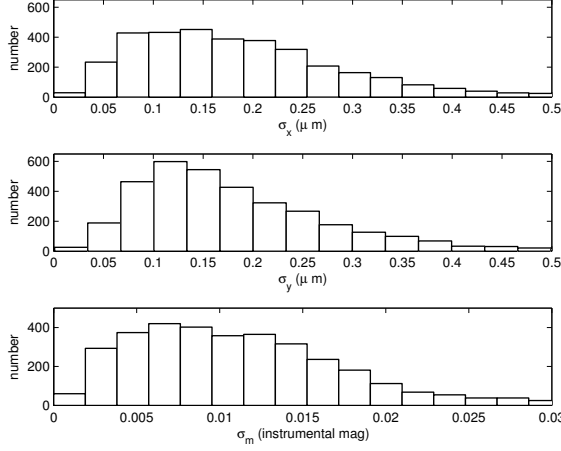
Table 1 lists the average values of the corresponding standard deviations. It can be seen that the results for digitizing repeatability in X and Y are almost the same. For the calibration plate, the position repeatability of the standard dots is about $0.03\ \mu\text{m}$ and the brightness repeatability is about 0.001 instrumental magnitude. For the astronomical plate, the position repeatability of stars is about $0.2\ \mu\text{m}$ and the brightness repeatability is about 0.01 instrumental magnitude. Considering the calculation error associated with centering and photometry for stars on the astronomical plate, the digitizing repeatability of the machine itself should be better than the above values in the measuring range.

3.3 Systematic Factors Affecting Digitizing Positions

The optical and mechanical components of the digitizer contain manufacturing errors, and there are also inevitably installation errors in the integration process of all components, which may introduce systematic effects in digitization results. These factors include: lens distortion, the actual optical resolution, non-linearity in the guide rails, non-uniformity in the linear motors that are part of the mobile platform, deviation of image mosaic (starting deviation in Y and overlapping deviation in X) and non-orthogonality between the scanning direction and the camera line array direction. According to their various representations, all these factors were evaluated and calibrated.

Table 1 Test Results of Digitizing Repeatability

Object	Measuring range (mm)	$\bar{\sigma}_x$ (μm)	$\bar{\sigma}_y$ (μm)	$\bar{\sigma}_m$ (mag)	Number of stars
Calibration plate	50×50	0.024	0.028	0.0001	40 359
Astronomical plate	288×288	0.175	0.169	0.01	3501

**Fig. 6** Histogram of the standard deviations of the residuals of the measured coordinates and brightnesses for all stars on the astronomical plate with a size of $300 \text{ mm} \times 300 \text{ mm}$.

3.3.1 Lens distortion

Digitization of an astronomical plate is equivalent to re-imaging of the original plate. In order to reduce imaging distortion, the digitizer is equipped with a doublesided telecentric lens. The lens has very low distortion that is better than 0.05% for the specified working size of 70.0 mm. The closer the center of the field of view is to what is being imaged, the smaller the lens distortion effect. It can be estimated that even a distortion of 0.01% can amount to a micron level for the linear array camera length of 28.8 mm. So, the lens distortion should not be ignored and needs to be calibrated. The effect of lens distortion on digitizing positions is reflected in the direction of the linear array camera, expressed in X . Therefore, for a digitized image of the calibration plate, we can fit the relationship between the theoretical and measured positions of all standard dots, and then investigate the distribution of residuals in X along X , as shown in the upper panel of Figure 7. It can obviously be shown that the influence of the lens distortion is symmetrically distributed on both sides of the center of field of view. The lens distortion becomes progressively larger with distance from the center of field of view, and the maximum is about

0.7 μm . In data processing, the digitized positions can be corrected according to calibration data on the lens distortion. The lower panel of Figure 7 shows the distribution of residuals after correction. Here the distribution has no systematic trend and the effect of lens distortion has been eliminated.

3.3.2 Optical resolution

The nominal magnification of the doublesided telecentric lens is 1:1, and the nominal physical size of the pixel in the linear array camera is 10 μm , so the theoretical optical resolution of the digitizer is 2540 DPI. In practice, the lenses are not perfect and there may be bias related to the physical size of pixels in the camera. The actual optical resolution of the digitizer should be calculated based on the digitized image of the calibration plate. Assuming ξ , η and x , y are the theoretical and measured coordinates of the standard dots on the calibration plate respectively, their relationship can be described as

$$\begin{cases} x = f \cos \theta \xi + f \sin \theta \eta + c, \\ y = -f \sin \theta \xi + f \cos \theta \eta + d, \end{cases} \quad (1)$$

where c , d and θ represent the translation and rotation between the theoretical and measured coordinate system, and f represents magnification. According to the calculation of standard dots, the digitizer has a magnification of 0.999844, and then the actual optical resolution is 2539.6 DPI.

3.3.3 Non-linearity of the guide rails and non-uniformity of the linear motors that are part of the mobile platform

Ideally, the mobile platform should drive the astronomical plate to perform strict uniform linear motion along the scanning direction. However, the bending of the guide rails and the installation error affect the linearity of the scanning motion, which will introduce errors in digitized positions in X . On the other hand, the accuracy of the linear motor affects the uniformity of speed in the scanning motion, which will introduce errors into digitized positions in Y . In order to estimate the non-linearity and

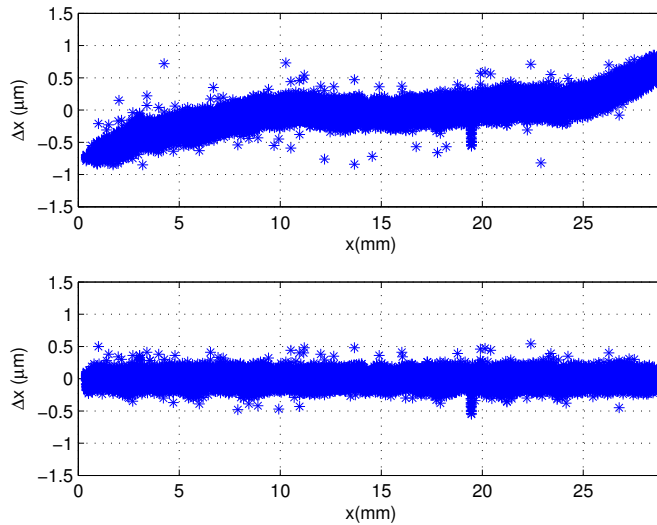


Fig. 7 Distribution of residuals in X along the direction of the linear array camera before (*top*) and after (*bottom*) correction for lens distortion.

non-uniformity quantitatively, we placed the calibration plate along the direction of scanning six times according to a step size of 50 mm, as shown in Figure 8.

The digitized images of the calibration plate in different locations are utilized to calculate the relationship between the theoretical and measured positions, and then used to investigate the systematic distribution of residuals in X and Y along Y , which reflects the influence of non-linearity in the guide rails and non-uniformity of the linear motors in each coverage range, as shown in Figures 9 and 10, respectively. It can be shown that the effect of non-linearity in the guide rails is mainly in a range of $0.4 \mu\text{m}$, and non-uniformity of the linear motors is in a range of $0.6 \mu\text{m}$.

3.3.4 Deviation of image mosaic

Limited by the optical lens and the linear array camera, the width of a single data acquisition is 28.8 mm. Since the side length of most astronomical plates exceeds 100 mm, each plate needs to be scanned many times to obtain multiple strip frames. Once all the strip frames from one plate have been recorded, they must be stitched into a mosaic image of the whole plate. The stitching process will introduce errors including starting deviation in Y and overlapping deviation in X , as shown in Figure 11.

In order to test the stitching error, we placed the calibration plate along X according to the step size of 28.8 mm, as shown in Figure 12. Every time the calibration plate was placed, it would cover two adjacent data

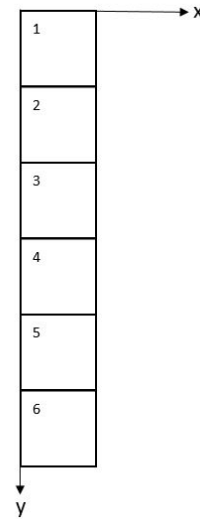


Fig. 8 Calibration plate was placed along Y six times according to a step size of 50 mm.

acquisition regions. According to the standard dots on the previous data acquisition region, the relationship between the measured and theoretical positions can be fitted. Then, the theoretical positions of the standard dots on the latter region were converted through the relationship and compared with their corresponding measured positions, so as to get starting and overlapping deviation of the two adjacent regions. Here, the starting deviation between the two adjacent regions is reflected in the relative shift in Y , and the overlapping deviation is reflected in the relative shift in X . We carried out five rounds of measurements and the results are presented in

Table 2 Measurement Results of the Starting Deviation of Two Adjacent Data Acquisition Regions

No.	Latter region relative to the previous one (μm)								
	2–1	3–2	4–3	5–4	6–5	7–6	8–7	9–8	10–9
1	-0.69	-0.34	-0.72	-0.22	-0.50	-0.49	-0.06	-0.66	-0.48
2	-0.58	-0.51	-0.52	-0.18	-0.42	-0.39	-0.16	-0.51	-0.57
3	-0.81	-0.27	-0.60	-0.22	-0.41	-0.59	0.09	-0.77	-0.53
4	-0.89	-0.22	-0.51	-0.26	-0.36	-0.65	0.02	-0.74	-0.57
5	-0.76	-0.35	-0.66	-0.33	-0.55	-0.51	-0.05	-0.71	-0.51
Mean	-0.75	-0.34	-0.60	-0.24	-0.45	-0.53	-0.03	-0.68	-0.53
σ	0.12	0.11	0.09	0.06	0.08	0.10	0.09	0.10	0.04

Table 3 Measurement Results of the Overlapping Deviation of Two Adjacent Data Acquisition Regions

No.	Latter region relative to the previous one (μm)								
	2–1	3–2	4–3	5–4	6–5	7–6	8–7	9–8	10–9
1	0.11	-1.59	0.04	-0.38	-1.16	0.17	-0.94	0.32	-1.45
2	0.03	-1.58	-0.04	-0.54	-1.26	0.07	-0.94	0.21	-1.48
3	0.20	-1.69	0.14	-0.42	-1.15	0.26	-1.08	0.48	-1.50
4	0.33	-1.89	0.23	-0.50	-1.05	0.22	-0.94	0.46	-1.48
5	0.28	-1.60	0.16	-0.68	-1.04	0.17	-1.03	0.29	-1.40
Mean	0.19	-1.67	0.11	-0.50	-1.13	0.18	-0.99	0.35	-1.46
σ	0.12	0.13	0.11	0.12	0.09	0.07	0.07	0.12	0.04

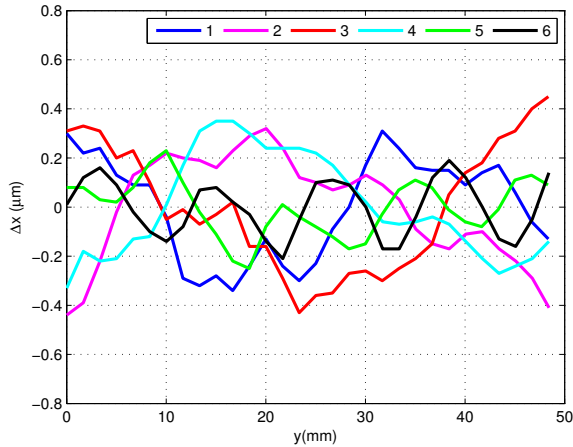


Fig. 9 Systematic distribution of the residuals in X along Y in the case of the calibration plate in different locations.

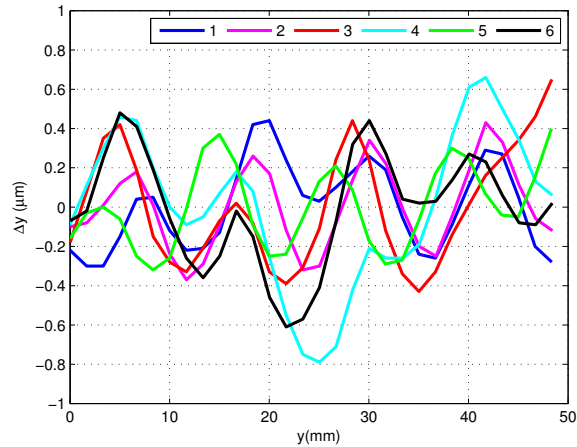


Fig. 10 Systematic distribution of the residuals in Y along Y in the case of the calibration plate in different locations.

Tables 2 and 3. It can be seen that each of the two adjacent regions has starting and overlapping deviation at the micron level, which would accumulate to a few microns from the first strip to the last. From multiple rounds of measurement, the starting and overlapping deviation is relatively stable and the repeatability is better than $0.15 \mu\text{m}$. Therefore, the mean value of deviation measurement can be regarded as compensation for the step motion of the mobile platform to reduce the influence of stitching error.

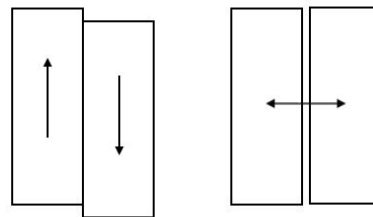


Fig. 11 Sketch map of starting deviation in Y and overlapping deviation in X.

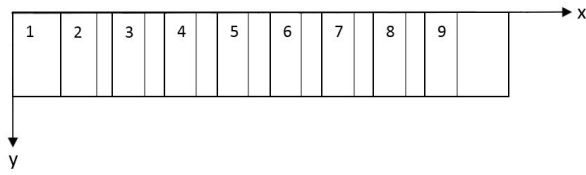


Fig. 12 Calibration plate was placed along X nine times according to a step size of 28.8 mm.

3.3.5 Non-orthogonality between scanning direction and camera line array direction

Line scanning requires that the scanning direction should be perpendicular to the direction of the linear array camera. However, there is some non-orthogonality between the two directions because of installation errors. The effect of non-orthogonality on digitizing positions in Y will reach a maximum at the edge of the field of view, which can be expressed formally as

$$\Delta y_{\max} = 0.5 \cdot l \cdot \tan \theta \quad (2)$$

where l represents the length of the linear array camera and θ represents the non-orthogonal angle. The following approach is adopted to evaluate non-orthogonality. For the digitized image of the calibration plate, two straight lines are obtained respectively by fitting the standard dots on each row and each column. The difference between the angle of the two lines and 90° can reflect the non-orthogonality between the scanning and the linear array camera direction. In the actual test, the digitized image contains 201 rows \times 100 columns of standard dots, which consists of 20 100 pairs of lines.

Figure 13 shows the distribution of the non-orthogonality results from all pairs of lines. It can be seen that the average value of non-orthogonality is about $1.25''$. In the case of the linear array camera with a length of 28.8 mm, the influence of non-orthogonality would be less than $0.17 \mu\text{m}$.

3.4 Comprehensive Test on the Precision of Digitizing Positions

The calibration plate provides a good reference for testing systematic factors affecting digitizing positions, but the size of the calibration plate is too small to cover the whole measuring range. So, we used a $300 \text{ mm} \times 300 \text{ mm}$ astronomical plate to carry out a comprehensive test on the precision of the digitized positions.

Though the positions of stars on the astronomical plate are not known exactly, the relative positions of all

Table 4 Standard deviations of the 0° with the 90° image and the 0° with the 180° image

No.	σ (μm)	
	$0^\circ - 90^\circ$	$0^\circ - 180^\circ$
1	0.79	0.87
2	0.76	0.84
3	0.75	0.86
4	0.75	0.87
5	0.79	0.84
6	0.79	0.88

the stars are fixed. With this advantage, the plate was digitized at different angles and the conversion residuals of the positions of common stars on different images were investigated. The specific measures are as follows: First, the plate was digitized to acquire its digitized image at 0° . Second, the plate was rotated 90° and 180° , respectively, and digitized again to acquire its image at 90° and 180° . Third, common stars were used to fit the 0° image with the 90° image and the 0° image with the 180° image, to remove systematic error between the images such as translation and rotation. Fourth, the residual distribution of the positions and the standard deviations were investigated.

Table 4 lists the standard deviations of six groups of tests. The conversion residuals of the positions between the 0° image and the 90° image, and between the 0° image and the 180° image are shown in Figures 14 and 15 respectively, where the plate is divided evenly into 20×20 blocks and each arrow represents the average value of the residuals within the block. It can be seen that the residual distribution does not show a significant systematic tendency; the standard deviation is better than $0.9 \mu\text{m}$. According to the principle of error transfer, here the standard deviation (expressed as σ) represents the comprehensive position error of the two images, which includes a digitizing error (expressed as σ_d) and a centroid error (expressed as σ_c), and it can be expressed formally as $\sigma^2 = 2 \cdot (\sigma_d^2 + \sigma_c^2)$, whereby the overall digitizing error σ_d caused by the machine is deduced to be better than $0.7 \mu\text{m}$.

4 CONCLUDING REMARKS

The vast majority of astronomical plates in China have not been digitized yet, which restricts the value of first hand observation data they might contain. The main component of the film on an astronomical plate is silver bromide and a change in the environment will make the film

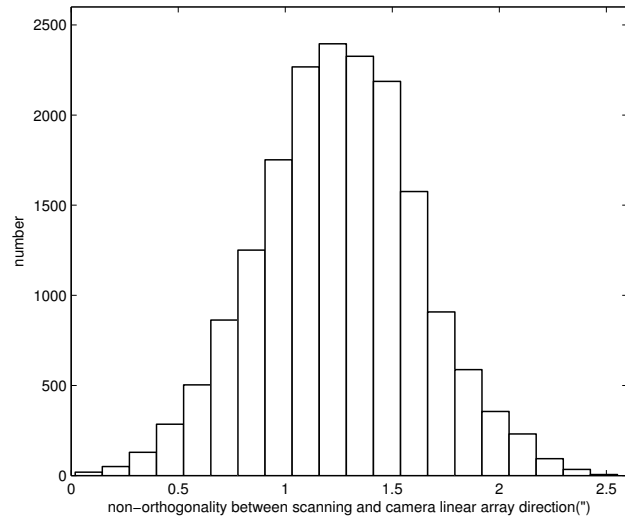


Fig. 13 Test of non-orthogonality between the scanning direction and the camera line array direction.

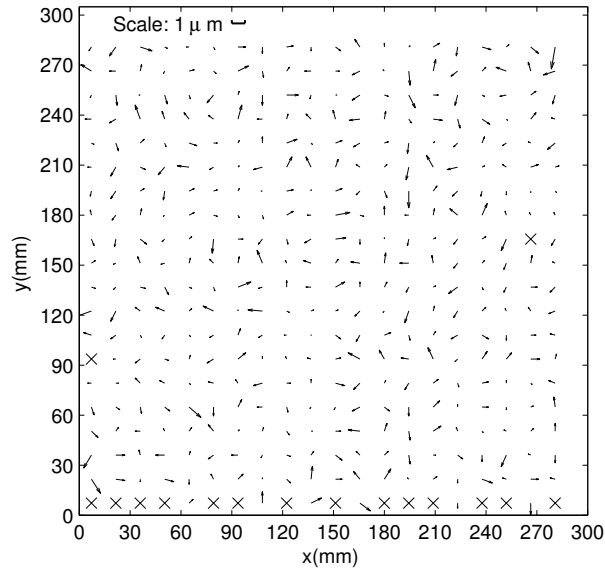


Fig. 14 Residual distribution between 0° image and 90° image, where “x” represents no common stars in a block.

become yellow, moldy or even fall off. Even if kept in an ideal environment with constant temperature and humidity, the film on the plate will gradually deteriorate as time goes on. Therefore, digitization of astronomical plates is of great significance for permanent preservation and full use of these valuable observation data. A digitizer with high precision and high measuring speed is a key piece of equipment to carry out the task of digitizing these astronomical plates.

Shanghai Astronomical Observatory and Nishimura Co., Ltd of Japan have jointly developed a new digitizer for glass astrophotographic plates. After two years of development, this machine provides digitization precision of better than $1\ \mu\text{m}$ in position, and 10 minutes are needed to measure a plate with a size of $300\ \text{mm} \times 300\ \text{mm}$, which meets the requirement for digitization of astronomical plates. In this paper, we describe the main structure and working mode of the digitizer, as well as the results of its performance test. The re-

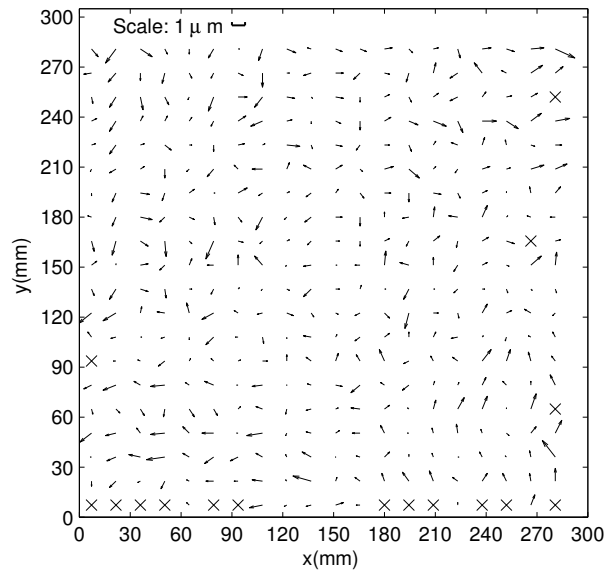


Fig. 15 Residual distribution between 0° image and 180° image, where “x” represents no common stars in a block.

sults show that the brightness uniformity of illumination within the measuring area is better than 0.15%, the repeatability of digitized positions is better than $0.2 \mu\text{m}$ and the repeatability of digitized brightness is better than 0.01 instrumental magnitude. The systematic factors affecting digitized positions are calibrated and evaluated. Based on an astronomical plate with a size of $300 \text{ mm} \times 300 \text{ mm}$, the overall measurement error of the digitizer is deduced to be better than $0.7 \mu\text{m}$.

At present, the digitization of the astronomical plates is being carried out by the digitizer and the digitization of all astronomical plates in China is expected to be completed in 2017. The digitized data are planned to be stored in the Chinese Virtual Observatory database and gradually be released to the international astronomical community.

Acknowledgements We would like to acknowledge the suggestions and assistance from Prof. Robert Simcoe, Jean-Pierre De Cuyper, Zi Zhu and Yong-Heng Zhao during the development of the digitizer. This work is supported by the National Science and Technology Basic Work (2012FY120500) and the National Natural Science Foundation of China (U1331112 and 11573055).

References

- de Cuyper, J.-P., & Winter, L. 2006, in *Astronomical Society of the Pacific Conference Series*, Vol. 351, *Astronomical Data Analysis Software and Systems XV*, eds. C. Gabriel, C. Arviset, D. Ponz, & S. Enrique, 587
- Fresneau, A., Argyle, R. W., Marino, G., & Messina, S. 2001, *AJ*, 121, 517
- Høg, E., Fabricius, C., Makarov, V. V., et al. 2000, *A&A*, 357, 367
- Kavelaars, J. 2004, *PDPP Newsletter*, 2, 22
- Mao, Y.-Q., Chen, J., Jiang, P.-F., & Zhuang, X.-J. 1993, *Acta Astronomica Sinica*, 34, 180
- Simcoe, R. J., Grindlay, J. E., Los, E. J., et al. 2006, in *Proc. SPIE*, Vol. 6312, *Society of Photo-Optical Instrumentation Engineers (SPIE) Conference Series*, 631217
- Torres, G., & Stefanik, R. P. 2000, *AJ*, 119, 1914
- Wang, J., Li, C., Zhao, J., & Jiang, P. 1996, *Acta Astronomica Sinica*, 37, 68
- Yan, L.-S., Hu, Z.-W., & Huang C.-C. 1986, *Chin. Sci. Bull.*, 17, 1325
- Yan, D., Qiao, R. C., Dourneau, G., et al. 2016, *MNRAS*, 457, 2900